Articles

The Adsorption of Perfluorooctane Sulfonate onto Sand, Clay, and Iron Oxide Surfaces

Ramona L. Johnson,[§] Amy J. Anschutz,[‡] Jean M. Smolen,[†] Matt F. Simcik,*[,§] and R. Lee Penn*[,‡]

Department of Chemistry, Saint Joseph's University, 5600 City Avenue, Philadelphia, Pennsylvania 19131, Department of Chemistry, University of Minnesota, 207 Pleasant Street SE, Minneapolis, Minnesota 55455, and Division of Environmental Health Sciences, School of Public Health, University of Minnesota, MMC 807, 420 Delaware Street SE, Minneapolis, Minnesota 55455

Fluorinated anionic surfactants have drawn considerable attention due to recent work showing significant concentrations in surface waters and biota from around the globe. A detailed understanding of the transport and fate of fluorinated surfactants through soil and like media must include an elucidation of mineral surface chemistry. Five materials were equilibrated with solutions of perfluorooctane sulfonate (PFOS) to characterize adsorption: kaolinite, Ottawa sand standard, synthetic goethite, Lake Michigan sediment, and iron-coated sand from Mappsville, VA. Aqueous and adsorbed PFOS was quantified with LC/MS (mass balance average: 101 ± 12 %, $n = 37$). The materials showed a near linear increase in adsorption as the equilibrium concentrations increased. Isotherms and calculated solid/solution distribution ratio experiments indicated that PFOS adsorption is significant but smaller than hydrocarbon analogues or organic compounds of similar molecular weight. Surface area normalized adsorption increased for the materials in the following order: goethite < kaolinite < high iron sand < Ottawa sand standard. Experimental results and comparisons to published data suggest that organic carbon may play an important role in sorption whereas electrostatic attraction may play a role when organic carbon is not present.

Introduction

Aqueous and mineral surface chemical behaviors are major controlling factors in the fate and transport of anthropogenic and natural chemical species. The widespread occurrence of perfluorinated surfactants both in animal tissue[1−7] and in surface waters[8−12] is an important environmental problem that requires a multifaceted approach to predicting their transport and fate. Many of these surfactants, such as PFOS (perfluorooctane sulfonate), are used in a wide range of applications, such as the production of polymers, greases, stain protectants, and lubricants.[1,8,13] In addition, these compounds are used extensively as foams for combating hydrocarbon fuel fires, in particular, fires associated with fuel spills. Furthermore, significant concentrations of fluorinated surfactants have been found in groundwater near fire-fighting training sites[14,15] and near a site at which a spill of 22 000 L of fire retardant foam containing perfluorinated surfactants occurred in June of 2000.[9] A detailed understanding of the transport and fate of fluorinated anionic surfactants in groundwater must include elucidation of the interaction of these molecules with mineral surfaces.

Previous work characterizing the change in forces of interaction between two bare silica surfaces in aqueous solution suggested that no specific adsorption of perfluorinated anionic surfactants occurred.[16] However, when the silica surfaces were modified using cationic surfactant, resulting in positively charged surfaces, specific binding of the perfluorinated anionic surfactants was observed.[16] Thus, we hypothesized that adsorption of PFOS to mineral surfaces will be controlled mostly by electrostatic forces. In addition, however, an increase in surfactant binding was observed for longer chain lengths in this previous work.[16] Thus, we further hypothesized that electrostatics will not be the only mechanism at work. In this work, we have quantified adsorption of perfluorooctanesulfonate onto four well-characterized natural materials (kaolinite, Ottawa sand, "iron oxide" coated sands, and sediment from Lake Michigan) and synthetic (goethite) particles.

Experimental

Chemical Reagents. Heptadecafluorooctanesulfonic acid potassium salt (PFOS) was acquired from Fluka. Potassium hydroxide, potassium nitrate, water (HPLC grade), and methanol (Optima grade) and $Fe(NO_3)_3 \cdot 9H_2O$ were obtained from Fisher. All chemicals were used as received and tested for PFOS contamination (except PFOS).

Solid Materials. The following solid materials were used as received in adsorption studies: Ottawa sand standard from Washington County, GA (Fisher, 20−30 mesh), kaolinite (high (KGa-2) and low (KGa-1b) defect), iron-coated sand from Mappsville, VA (reference sediment AH4-304-87998). All solid materials were extracted with methanol to check for PFOS contamination prior to use in the adsorption studies; none was

* To whom correspondence should be addressed. (M.F.S.) phone: 612-626-6269, fax: 612-626-0650, e-mail: msimcik@umn.edu; (R.L.P.) phone: 612-626-4680, e-mail: penn@chem.umn.edu.
† Saint Joseph's University.
‡ Department of Chemistry, University of Minnesota.
§ School of Public Health, University of Minnesota.

10.1021/je060285g CCC: $37.00
Published on Web 05/08/2007

Table 1. Material Characteristics and Sorption Coefficients[a]

material	K_d L/kg	f_{OC}	log K_{OC} L/kg	surface area m^2/g	pH_{zpc}	charge
Ottawa sand	2.81	0[36]		$2 \cdot 10^{-3}$	2.5[37]	−
kaolinite	5.31	0.02[36]	2.4	10	4.6[37]	−
Lake Michigan sediment	7.52	0.02−0.03[38]	2.4−2.6			
goethite	7.88	0		58	7.5−9.5[39−41]	+
high iron sand	8.90			6		±[28]
clay	18.3[34]	0.03[34]	2.8[c]			
clay loam	9.72[34]	0.03[34]	2.6[c]			
sandy loam	35.3[34]	0.03[34]	3.1[c]			
river sediment	7.42[34]	0.0[34]	2.8[c]			
POTW	120[34]	0.4[b]	2.5[c]			

[a] Values with references are literature values. [b]Calculated from K_d and f_{OC}. [c]Estimated from Metcalf and Eddy.[35]

detected. Table 1 summarizes the geometric or measured surface areas for each of these natural materials.

Goethite particles were prepared using a method adapted from Schwertmann and Cornell.[17] Using a glass-coated magnetic stir rod to achieve efficient stirring, 41.95 g of $Fe(NO_3)_3 \cdot 9H_2O$ was added to 900 mL of HPLC grade H_2O. While stirring, the pH was adjusted to 12.8 using 5 M KOH in a 1 L Nalgene polyethylene bottle. A deep maroon suspension formed. The suspension was placed in an oven at 90 °C with the cap slightly loose for 6 days. After heating, a yellow-orange precipitate was present. The goethite suspension was split into six 50 mL centrifuge tubes and centrifuged at 6000 rpm for 5 to 10 min intervals. The supernatant was discarded after each wash, and the goethite was resuspended using HPLC grade water. This process was repeated six times, after which the supernatant pH was 7. The goethite was resuspended in HPLC grade water and used in adsorption experiments as a 15.7 g/L slurry. A dried sample of this goethite was extracted with methanol to check for PFOS contamination prior to use in the adsorption studies; none was detected.

Solids Analysis. Goethite samples were characterized using TEM and X-ray diffraction (XRD). TEM images demonstrated that the goethite crystals were acicular with average dimensions of 28 nm × 346 nm. The geometric surface area was calculated using the particle size and size distribution data obtained from TEM images and the known crystallography of goethite (as described by Anschutz and Penn[18]) and found to be 58 m^2/g (Table 1).

PFOS Contamination Check. All solids, natural and synthetic, and each type of plasticware, filter, and other similar types of supplies employed were extracted with methanol to verify that these items contained no measurable PFOS; none was detected.

Adsorption Experiments. Adsorption experiments were conducted using 15 mL high-density polyethylene centrifuge tubes. Solid materials (10 to 80 mg) were massed into each tube before the addition of water. Potassium nitrate was then added in concentrations ranging from 0.01 to 0.1 M to fix the ionic strength. To aqueous suspensions of the solids was added a small volume of stock aqueous PFOS solution. The final volume of each suspension was controlled so that it was consistent for each experiment. For the pH dependence experiments, initial PFOS concentrations were 1.13 ppm. This value is significantly below the expected hemi-micelle concentration (hmc). Shinoda et al. concluded that the critical micelle concentration (cmc) was mostly dependent on chain length and not counterion and reported a cmc of 6.3 mM (3.2 %) for $C_8F_{17}SO_3Li$.[19] Schwarzenbach et al. state that hemi-micelles are most likely to form in the range of 0.001 to 0.01 of the cmc.[20] Therefore, one would not expect hemi-micelle formation for PFOS at 1 ppm. Suspension pHs were adjusted and determined using a VWR Symphony electrode. Initial PFOS concentrations for the isotherm experiments ranged from 0.12 to 8.0 ppm. PFOS/solid suspensions were equilibrated for 22 to 24 h. This duration was sufficient to equilibrate the suspensions and allowed for complete extraction, as shown by the mass balances and a separate equilibration experiment which showed no statistical ($p < 0.05$) change in adsorption from 24 to 72 h. After this time, tubes were centrifuged at 3000 rpm for 15 min using an Eppendorf 5804 centrifuge. After centrifugation, the supernatant was passed through a 25 mm, 0.2 μm Millipore nylon filter into a clean centrifuge tube. The aqueous filtrate was diluted using the appropriate amount of HPLC grade water for LC/MS analysis.

To extract the adsorbed PFOS from the solids, 10 mL of Optima grade methanol was added to the remaining solid material in the tube. The small mass of solids collected on the filter would not have altered the results if included in the extraction. Solid suspensions were agitated using a Vortexer and/or a wrist action shaker and then sonicated for 30 min. The total contact time of the methanol with the solid materials was 1 to 3 h. Methanol suspensions were centrifuged at 3000 rpm for 10 min. The supernatant was passed through a 25 mm, 0.2 μm Millipore nylon filter into a clean centrifuge tube. The methanol filtrate was diluted in the appropriate amount of Optima grade methanol for LC/MS analysis.

LC/MS Analysis. Samples for LC/MS analysis were placed into Wheaton glass vials and crimp-sealed with natural rubber septa (Chrom Tech Inc., Apple Valley, MN). Methanol blanks were run between each sample and standard injection. The detector was operated in selective ion monitoring (SIM) mode at the PFOS parent ion of 499 amu. The ion extracted at this mass unit was used to determine the peak areas for the PFOS standards and the analytical samples.

Analyte separation was achieved using a Hewlett-Packard model 1090 high-performance liquid chromatograph. Methanol calibration standards and extracts were injected (1 μL) onto a 50 × 1 mm (3 μm) Luna C_{18} analytical column. A guard column (Security Guard, C_{18}, Phenomenex, Torrenc, CA) is placed in front of the analytical column. The flow rate was maintained at 50 μL/min with a mobile phase of 2 mmol of ammonium acetate in 70 % HPLC-grade water, 30 % methanol (A), and 2 mmol of ammonium acetate in methanol (B). The gradient starts at 100 % A transferring to 57.1 % B over the first 13 min, is held at 57.1 % B until 18 min, transferred to 100 % B at 33 min, held at 100 % B until 36 min, transferred to 100 % A over the next minute, and held at 100 % A until 45 min. The column temperature was maintained at 38 °C.

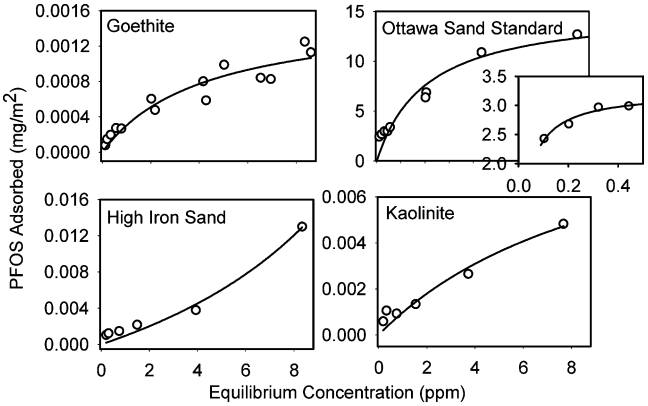

Figure 1. Langmuir adsorption isotherms of PFOS onto goethite, Ottawa sand, high iron sand, and kaolinite.

Detection of perfluorinated compounds was performed using a Hewlett-Packard 1100 series mass spectrometer operating in electrospray negative ionization mode. Detection parameters were optimized for the $[M]^-$ ion of PFOS ($m/z = 499$). For this, the fragmentor voltage was maintained at 70 V, and the capillary voltage was maintained at 4000 V. Quantification was performed using a four point external standard calibration curve with concentrations of approximately 5, 25, 50, and 100 ng/mL of PFOS. The 5 ng/mL standard is higher than the instrument detection limit.[12]

PFOS Charge Calculation. Gas-phase molecular geometries for the conjugate base forms of octanesulfanoic acid and PFOS were optimized at the B3LYP[21−24] level of density functional theory[25] using the 6-31G(d) basis set.[26] Atomic partial charges were computed from Mulliken population analysis,[27] which is a particularly efficient means for the analysis of qualitative trends in charge distributions.[25]

Results and Discussion

Figure 1 shows the adsorption isotherms for PFOS adsorbed onto goethite, Ottawa sand, high iron sand, and kaolinite. The amount of PFOS adsorbed per unit surface area is plotted as a function of the equilibrium aqueous PFOS concentration. Mass balances were calculated for each experiment, and the average mass balance for all the isotherm data was 101 % (std deviation 12 %, $n = 37$). Adsorption isotherms for adsorption of PFOS onto the solid materials were fit using linear, Langmuir, and Freundlich models, and all three gave acceptable results (fits are shown in Supporting Information). For simplicity, only the Langmuir model fits are presented (Figure 1) and discussed here. Surface area normalized adsorption of PFOS is greatest for Ottawa sand standard, then high iron sand, kaolinite, and least for goethite. These differences can be seen clearly in Figure 1 by noting the different *y*-axes. For each of these solids, the amount of PFOS adsorbed increases as the equilibrium concentration increases, which is as expected. For both goethite and Ottawa sand, adsorption appears to approach saturation as the equilibrium concentration nears 8 ppm, indicating the possibility that a monolayer of coverage has been achieved. Converting the mass of PFOS adsorbed at saturation per meter squared to the number of PFOS molecules adsorbed per unit surface area results in 10 PFOS molecules/nm^2 of Ottawa sand, $1.4 \cdot 10^{-3}$ PFOS molecules/nm^2 of goethite, and $6.0 \cdot 10^{-3}$ PFOS molecules/nm^2 of kaolinite. Results clearly demonstrate that the nature of the mineral surface strongly influences the degree of adsorption. On the basis of the molecule size, the number of PFOS molecules per unit surface area for a monolayer of coverage is estimated to range from $2 \cdot 10^1$ molecules/nm^2 if the long axis of the molecule is normal to the surface to only 4 molecules/nm^2 if the long axis of the molecule is parallel to the surface, assuming no space between molecules. This result suggests that a monolayer of coverage on Ottawa sand standard is exceeded at a concentration well below the apparent saturation concentration. In the sub-2 ppm portion of the adsorption isotherm, the leveling off of the data at approximately 0.4 ppm aqueous PFOS may be consistent with the formation of a monolayer of coverage. Estimating the monolayer capacity by performing a Langmuir fit of the first four points (shown in the inset to the upper right-hand graph in Figure 1) yields a result of 3 mg/m^2, which is consistent with approximately 4 molecules/nm^2 adsorbed. This level of coverage is consistent with a monolayer where the long axis is parallel to the surface. This conformation may be expected from the hydrophobicity of the perfluorinated tail of PFOS because at low levels of surface coverage (before a monolayer is achieved) this would minimize water−fluorine interactions.

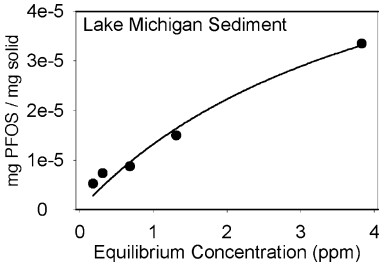

Figure 2. Langmuir adsorption isotherm of PFOS onto Lake Michigan sediment.

Finally, high iron sand represents a contrast to the other three materials in that the shape of the isotherm is consistent with multilayer adsorption despite the fact that the initial saturation at 4 ppm is well below a realistic monolayer of surface coverage ($5.0 \cdot 10^{-3}$ PFOS molecules/nm^2). In the cases of PFOS adsorption onto high iron sand, the surface area normalized adsorption is substantially lower than the degree of adsorption onto Ottawa sand standard and significantly higher than adsorption onto goethite and kaolinite. High iron sand is mostly quartz sand grains that are coated with nanomaterials predominantly composed of Al- and Si-rich phases and interspersed with agglomerates of goethite nanoparticles (commonly referred to as iron oxide coating).[28] On the basis of the data presented above, which demonstrated a higher affinity for quartz than for goethite or kaolinite, we hypothesize that the accessible/exposed quartz surface area, which is severely limited due to the coatings, is responsible for the apparent saturation in adsorption at 3 to 4 ppm aqueous PFOS. The contribution to PFOS absorptivity by the Al- and Si-rich materials and the iron oxides is expected to be comparatively small based on the results for kaolinite ($AlSi_2O_5$) and goethite (α-FeOOH).

Figure 2 shows the adsorption isotherm for the adsorption of PFOS onto Lake Michigan sediment. In this case, the adsorption is normalized to mass because attempts to quantify surface area by BET analysis failed. As in adsorption isotherms for goethite and kaolinite, the adsorption of PFOS to Lake Michigan plateaus, suggesting that adsorption may be approaching saturation (Figure 2). To compare the relative adsorption to all materials, solid/solution distribution coefficients, K_d, were calculated from the adsorption experiments

$$K_d = \frac{\text{mg of PFOS/kg of solid}}{\text{mg of PFOS/L of water}} = \frac{\text{L}}{\text{kg}} \quad (1)$$

K_d values in this study range from 2.8 to 8.9 L/kg. This range

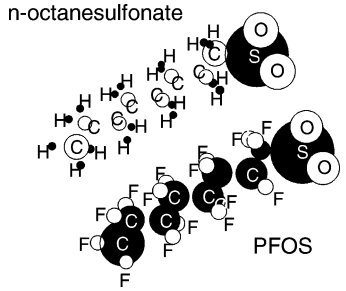

Figure 3. Atomic charges on *n*-octanesulfonate and PFOS. Black spheres are positively charged, and white spheres are negatively charged. The size of the sphere indicates the relative charge on each atom.

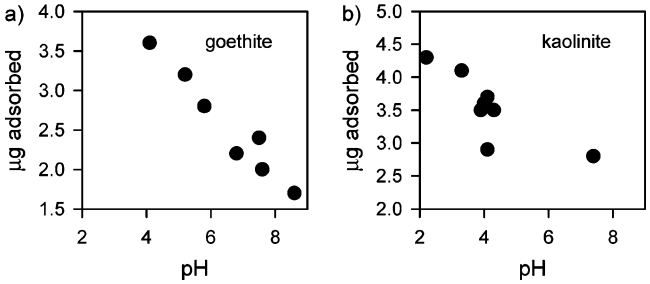

Figure 4. (a) Mass PFOS adsorbed onto goethite as a function of pH in equilibrated and unbuffered aqueous solutions. (b) Mass PFOS adsorbed onto kaolinite as a function of pH in equilibrated and unbuffered solutions. Initial concentration of added PFOS was 1.1 μg/mL for all solids. Mass balances ranged between 82 and 100 %. The pH values indicated on the *x*-axis are the experimental pH values after equilibration for 22 to 24 h.

of K_d values found for PFOS is lower than for many persistent organic pollutants of similar molecular weight, indicating a greater tendency to stay in the aqueous phase than compounds such as PCB congeners (log K_d range of 4 to 6). However, given the varied nature of groundwater saturated zones where the solids to water ratio (denoted by the bulk density to porosity ratio, ρ_b/n) can vary from 1 to 10 kg/L,[20] 74 to 99 % of the PFOS could be adsorbed onto solid surfaces in a groundwater system containing parts per million levels of PFOS and solid materials similar to those in this study.

The physical chemical properties of PFOS are not well characterized. Investigations to date are not always reliable due to the unpredictable nature of the compound. However, the critical micelle concentrations ($4.0 \cdot 10^3$ mg/L[29] and $3.2 \cdot 10^3$ mg/L[19]) indicate that in our experiments PFOS will be dissolved in the water phase; there is little potential of micelle formation, but it is possible that we have hemi-micelle formation above 3 ppm according to Schwarzenbach et al.[20] The relatively large acid dissociation constant of perfluorooctane sulfonic acid means that the dominant form in near surface and surficial waters will be the deprotonated form. Thus, we hypothesized that adsorption onto mineral surfaces would be dominated by electrostatic attraction between the negatively charged PFOS head group (i.e., the sulfonate) and the positively charged mineral surfaces. The charged nature of PFOS can be essentially described as a shell of negative charge around a core of positive charge (Figure 3). Density functional calculations of the gas-phase partial atomic charges for the oxygen atoms in octanesulfonate and PFOS indicate that the negative charges on the three oxygen atoms in the latter are smaller by about 0.05 atomic charge units each as compared to the former (see Supporting Information). Furthermore, the charges on the fluorine atoms are negative compared to the positive charges on hydrogen atoms on the hydrocarbon analogue (Figure 3). This results in a negative surface charge on the entire PFOS molecule. These results are consistent with the inductive effect expected for the electron-withdrawing fluorine atoms present in PFOS. Therefore, electrostatic interactions would not be limited solely to the sulfonate group.

Our hypothesis can be tested by qualitatively comparing the expected surface charge of each material and the experimental PFOS adsorption isotherms. The overall surface charge on a mineral surface is determined by the density of positively, neutrally, and negatively charged surface sites, and the distribution of those charges is dependent on pH. For silica, the charge density ranges from -0.0165 C/m^2 at pH 7.7 to -0.0046 C/m^2 at pH 5.9.[30] For goethite, the charge density ranges from 0.0024 C/m^2 at pH 8.5 to 0.078 C/m^2 at pH 5.[31] The pH of zero point charge, pH_{zpc}, for each material ranges from 2.5 to 9 (Table 1). On average, this means that Ottawa sand and kaolinite particles are expected to be negatively charged and goethite particles are expected to be positively charged at neutral pH. Although no pH_{zpc} is available for high iron sand, it is expected to have both positive and negative charges on the basis of its reported mineralogy.[28] The surface normalized adsorption trend observed is contrary to the electrostatic hypothesis. For those materials with no organic fraction, adsorption per unit surface increases with increasing negative charge (Figure 1, Table 1), which does not support the electrostatic argument.

The electrostatic hypothesis was further tested by performing single-point adsorption experiments with goethite and kaolinite as a function of solution pH in low ionic (0.01−0.1 M KNO_3), unbuffered solutions. When adsorption is controlled by electrostatics, as the average mineral surface charge decreases, the amount of adsorption is expected to decrease. As pH is increased, the average surface charge on the mineral particles becomes less positive. In the case of goethite, the particles are positively charged below a pH of approximately 8. In the case of kaolinite, using the pH_{zpc} estimates of 4 for basal surfaces and 7 for edge surfaces,[32] one would expect positive edge and basal surfaces below a pH of 4, positive edge and negative basal surfaces for pHs between 4 and 7, negatively charged basal surfaces in neutral pH solutions, and negative edge and basal surfaces above a pH of 7. Therefore, adsorption to both goethite and kaolinite should be expected to decrease as pH increases. PFOS adsorption on goethite was in fact reduced from 32 % at pH 4.1 to 16 % at pH 8.6 (Figure 4a). PFOS adsorption on kaolinite was also reduced from 39 % at pH 2.2 to 26 % at pH 7.4 (Figure 4b). The charges on goethite and kaolinite yield a reasonable explanation for the effect observed: as the pH increases, modest decreases in adsorption are observed. That is to say, when the particles are positively charged, greater adsorption is observed, and the results support the electrostatic argument.

Surfactants have the potential to sorb to surfaces as hemi-micelles rather than as individual molecules. At the concentrations used in these experiments, hemi-micelle adsorption could be expected (0.1 to 1.0 % of the critical micelle concentration).[33] However, the start of hemi-micelle adsorption is normally indicated as a normal adsorption isotherm at low concentrations and then a sharp increase in adsorption at hemi-micelle concentrations. Although none of the materials examined clearly displayed such activity, PFOS adsorption to high iron sand exhibits a slight upward curvature to its isotherm, and the molecular density of PFOS on the surface of Ottawa sand standard may indicate hemi-micelle formation or multilayer adsorption (Figure 1). Because of a lack of rapid increases in isotherms, we conclude it is unlikely that hemi-micelle adsorption is occurring, although there are insufficient data to be conclusive. This may be consistent with the repulsive interac-

tions of the negative surface charge on the entire PFOS molecule (Figure 3).

Given the ambiguous results supporting and arguing against electrostatic interactions, it is helpful to look at other possible mechanisms. Typically, for hydrophobic organic compounds, K_d values are correlated with the organic fraction of the solid material because such compounds tend to partition to the organic matter. However, most of the materials from this study have little or no associated organic matter. One study[34] reported a K_d value for PFOS and publicly owned treatment works (POTW) sludge that is an order of magnitude greater than those observed for other materials reported in that and this study (Table 1). This greater magnitude of K_d may be explained by the higher organic carbon content of sludge. Assuming a value of 75 % organic matter in activated sludge and 53 % organic carbon, we estimate that this POTW sludge has an f_{OC} of approximately 0.4.[35] In fact, for materials with measurable organic carbon fractions, normalizing the experimental distribution coefficient to the organic carbon content results in similar values (i.e., (3 to 7)·10^2 with one outlier at 13·10^2). This is surprising given the oleophobic nature of PFOS, although these K_{OC} values are still approximately 5 orders of magnitude lower than K_{OC} values for PCBs. These comparisons of the surface area normalized adsorption, the "inorganic" distribution coefficients, and the "organic" distribution coefficients suggest that both the inorganic and organic materials will influence fate and transport of PFOS in a groundwater system.

The effect of solution pH on adsorption of PFOS onto goethite and kaolinite points to the likelihood that adsorption is at least partially controlled by electrostatics. In contrast, the ranking of the mineral samples in order of decreasing surface area normalized adsorption does not agree with the electrostatic prediction: Ottawa sand standard > goethite ~ high iron sand > kaolinite. In addition, for samples containing organic carbon, there is a large range in f_{OC} (0.03 to 0.4) but a relatively small range in K_{OC} (Table 1). Comparisons of the surface area normalized adsorption, the inorganic distribution coefficients, and the organic distribution coefficients lead us to conclude that both the inorganic and organic materials will influence fate and transport of PFOS in a groundwater system but that the interaction between PFOS and the organic fraction is likely to be important. This conclusion is supported by the recent article of Higgins and Luthy, who concluded that both partitioning to organic carbon and electrostatic effects are important in the adsorption of perfluorinated surfactants.[42]

Supporting Information Available:

Tables showing the atomic charges on *n*-octanesulfonate and PFOS, Mulliken atomic charges, and regression coefficients and parameters for model fits and Figures S1 and S2. This material is available free of charge via the Internet at http://pubs.acs.org.

Literature Cited

(1) Giesy, J. P.; Kannan, K. Global distribution of perfluorooctane sulfonate in wildlife. *Environ. Sci. Technol.* **2001**, *35* (7), 1339−1342.

(2) Kannan, K.; Koistinen, J.; Beckmen, K.; Evans, T.; Gorzelany, J. F.; Hansen, K. J.; Jones, O. P. D.; Helle, E.; Nyman, M.; Giesy, J. P. Accumulation of perfluorooctane sulfonate in marine mammals. *Environ. Sci. Technol.* **2001**, *35* (8), 1593−1598.

(3) Kannan, K.; Franson, J. C.; Bowerman, W. W.; Hansen, K. J.; Jones, P. D.; Giesy, J. P. Perfluorooctane sulfonate in fish-eating water birds including bald eagles and albatrosses. *Environ. Sci. Technol.* **2001**, *35* (15), 3065−3070.

(4) Kannan, K.; Corsolini, S.; Falandysz, J.; Oehme, G.; Focardi, S.; Giesy, J. P. Perfluorooctanesulfonate and Related Fluorinated Hydrocarbons in Marine Mammals, Fishes, and Birds from Coasts of the Baltic and the Mediterranean Seas. *Environ. Sci. Technol.* **2002**, *36* (15), 3210−3216.

(5) Kannan, K.; Newsted, J.; Halbrook, R. S.; Giesy, J. P. Perfluorooctanesulfonate and Related Fluorinated Hydrocarbons in Mink and River Otters from the United States. *Environ. Sci. Technol.* **2002**, *36* (12), 2566−2571.

(6) Kannan, K.; Hansen, K. J.; Wade, T. L.; Giesy, J. P. Perfluorooctane Sulfonate in Oysters, Crassostrea virginica, from the Gulf of Mexico and the Chesapeake Bay, U.S.A. *Arch. Environ. Contam. Toxicol.* **2002**, *42* (3), 313−318.

(7) Kannan, K.; Choi, J.-W.; Iseki, N.; Senthilkumar, K.; Kim, D. H.; Masunaga, S.; Giesy, J. P. Concentrations of perfluorinated acids in livers of birds from Japan and Korea. *Chemosphere* **2002**, *49* (3), 225−231.

(8) Moody, C. A.; Kwan, W. C.; Martin, J. W.; Muir, D. C. G.; Mabury, S. A. Determination of Perfluorinated Surfactants in Surface Water Samples by Two Independent Analytical Techniques: Liquid Chromatography/Tandem Mass Spectrometry and 19F NMR. *Anal. Chem.* **2001**, *73* (10), 2200−2206.

(9) Moody, C. A.; Martin, J. W.; Kwan, W. C.; Muir, D. C. G.; Mabury, S. A. Monitoring Perfluorinated Surfactants in Biota and Surface Water Samples Following an Accidental Release of Fire-Fighting Foam into Etobicoke Creek. *Environ. Sci. Technol.* **2002**, *36* (4), 545−551.

(10) Boulanger, B.; Vargo, J.; Schnoor, J. L.; Hornbuckle, K. C. Detection of Perfluorooctane Surfactants in Great Lakes Water. *Environ. Sci. Technol.* **2004**, *38* (15), 4064−4070.

(11) Schultz, M. M.; Barofsky, D. F.; Field, J. A. Quantitative Determination of Fluorotelomer Sulfonates in Groundwater by LC MS/MS. *Environ. Sci. Technol.* **2004**, *38* (6), 1828−1835.

(12) Simcik, M. F.; Dorweiler, K. J. A Ratio of Perfluorochemical Concentrations as a Tracer of Atmospheric Deposition to Surface Waters. *Environ. Sci. Technol.* **2005**, *39*, 8678−8683.

(13) Moody, C. A.; Field, J. A. Perfluorinated Surfactants and the Environmental Implications of Their Use in Fire-Fighting Foams. *Environ. Sci. Technol.* **2000**, *34* (18), 3864−3870.

(14) Moody, C. A.; Field, J.; Strauss, S.; Hebert, G.; Odom, M. Occurrence and distribution of perfluorinated surfactants in groundwater impacted by fire-fighting activity. In *Book of Abstracts*, 219th ACS National Meeting, San Francisco, CA, March 26−30, 2000; American Chemical Society: Washington, DC, 2000; ENVR-027.

(15) Moody, C. A.; Field, J. A. Determination of Perfluorocarboxylates in Groundwater Impacted by Fire-Fighting Activity. *Environ. Sci. Technol.* **1999**, *33* (16), 2800−2806.

(16) McNamee, C. E.; Matsumoto, M.; Hartley, P. G.; Mulvaney, P.; Tsujii, Y.; Nakahara, M. Interaction Forces and Zeta Potentials of Cationic Polyelectrolyte Coated Silica Surfaces in Water and in Ethanol: Effects of Chain Length and Concentration of Perfluorinated Anionic Surfactants on Their Binding to the Surface. *Langmuir* **2001**, *17* (20), 6220−6227.

(17) Schwertmann, U.; Cornell, R. M. *Iron Oxides in the Laboratory*, 2nd ed.; Wiley−VCH: Weinheim, 2000; p 154.

(18) Anschutz, A. J.; Penn, R. L. Reduction of crystalline Iron(III) oxidyhydroxides using hydroquinone: Influence of phase and particle size. *Geochem. Trans.* **2005**, *6*, 60−66.

(19) Shinoda, K.; Hato, M.; Hayashi, T. The Physicochemical Properties of Aqueous Solutions of Fluorinated Surfactants. *J. Phys. Chem.* **1972**, *76* (6), 909−914.

(20) Schwarzenbach, R. P.; Gschwend, P. M.; Imboden, D. M. *Environmental Organic Chemistry*, 2nd ed.; John Wiley & Sons: New York, 2003.

(21) Becke, A. D. Density-functional exchange-energy approximation with correct asymptotic behavior. *Phys. Rev. A: At., Mol., Opt. Phys.* **1988**, *38* (6), 3098−3100.

(22) Becke, A. D. Density-functional, thermochemistry. III. The role of exact exchange. *J. Chem. Phys.* **1993**, *98* (7), 5648−5652.

(23) Lee, C.; Yang, W.; Parr, R. G. Development of the Colle−Salvetti correlation-energy formula into a functional of the electron density. *Phys. Rev. B: Condens. Matter Mater. Phys.* **1988**, *37* (2), 785−789.

(24) Stephens, P. J.; Devlin, F. J.; Chabalowski, C. F.; Frisch, M. J. Ab Initio Calculation of Vibrational Absorption and Circular Dichroism Spectra Using Density Functional Force Fields. *J. Phys. Chem.* **1994**, *98* (45), 11623−11627.

(25) Cramer, C. J., *Essentials of Computational Chemistry*, 2nd ed.; John Wiley & Sons: Chichester, 2004; p 596.

(26) Hehre, W. J.; Radom, L.; Schleyer, P. v.; Pople, J. A. *Ab Initio Molecular Orbital Theory*; Wiley: New York, 1986.

(27) Mulliken, R. S. Electronic population analysis on LCAO−MO [linear combination of atomic orbital−molecular orbital] molecular wave functions. I. *J. Chem. Phys.* **1955**, *23*, 1833−1840.

(28) Penn, R. L.; Zhu, C.; Xu, H.; Veblen, D. R. Iron oxide coatings on sand grains from the Atlantic Coastal Plain: High-resolution transmission electron microscopy characterization. *Geology* **2001**, *29* (9), 843−846.

(29) Kissa, E. Fluorinated Surfactants: Synthesis-Properties-Applications. [In: *Surfactant Sci. Ser.* **1994**, *50*] 1994; p 469.
(30) Ahmed, S. M. Dissociation of oxide surfaces at the liquid−solid interface. *Can. J. Chem.* **1966**, *44* (14), 1663−70.
(31) Lumsdon, D. G.; Evans, L. J. Surface complexation model parameters for Goethite (α-FeOOH). *J. Colloid Interface Sci.* **1994**, *164* (1), 119−125.
(32) Palomino, A. M.; Santamarina, J. C. Fabric map for kaolinite: Effects of pH and ionic concentration on behavior. *Clays Clay Miner.* **2005**, *53* (3), 211−223.
(33) Schwarzenbach, R. P.; Gschwend, P. M.; Imboden, D. M. *Environmental Organic Chemistry*; John Wiley & Sons: New York, 1993.
(34) Ellefson, M. *Soil adsorption/desorption study of potassium perlfluorooctane sulfonate (PFOS)*; EPA Docket AR226-1030a030; 3M Company: Maplewood, MN, 2001.
(35) Tchobanoglous, G.; Burton, F. L. *Metcalf & Eddy: Wastewater Engineering*; McGraw-Hill, Inc.: New York, 1991.
(36) Moore, R. S.; Taylor, D. H.; Sturman, L. S.; Reddy, M. M.; Fuhs, G. W. Poliovirus adsorption by 34 minerals and soils. *Appl. Environ. Microbiol.* **1981**, *42* (6), 963−975.
(37) Kaplan, D. I. Influence of surface charge of an Fe-oxide and an organic matter dominated soil on iodide and pertechnetate sorption. *Radiochim. Acta* **2003**, *91* (3), 173−178.
(38) Golden, K. A. Organochlorines in Lake Michigan Sediments. Master of Science, University of Minnesota, Minneapolis, Minnesota, 1994.
(39) Cornell, R. M.; Schwertmann, U. *The Iron Oxides: structure, properties, reactions, occurences, and uses*, 2nd ed.; Wiley-VCH: Weinheim, 2003.
(40) Gaboriaud, F.; Ehrhardt, J.-J. Effects of different crystal faces on the surface charge of colloidal goethite (α-FeOOH) particles: an experimental and modeling study. *Geochim. Cosmochim. Acta* **2003**, *67* (5), 967−983.
(41) Kosmulski, M. A literature survey of the differences between the reported isoelectric points and their discussion. *Colloids Surf., A* **2003**, *222* (1−3), 113−118.
(42) Higgins, C. P.; Luthy, R. G. Sorption of Perfluorinated Surfactants on Sediments. *Environ. Sci. Technol.* **2006**, *40* (23), 7251−7256.

Received for review June 21, 2006. Accepted March 25, 2007.

JE060285G